Molecule/quantum dot orbital hybridisation harnesses endothermic singlet exciton fission

Jie Zhang [1], Hayato Sakai [2]*, Katsuaki Suzuki [1], Ramsha Khan [3], Taku Hasobe [2], I-Ya Chang [4], Kim Hyeon-Deuk [5]*, Hironori Kaji [1] & Masanori Sakamoto [1,6]*

[1]Institute for Chemical Research, Kyoto University, Gokasho, Uji, Kyoto 611-0011, Japan

[2] Department of Chemistry, Faculty of Science and Technology, Keio University, 3-14-1 Hiyoshi, Kohoku-ku, Yokohama, Kanagawa 223-8522, Japan

[3]Chemistry and Advanced Materials Group, Faculty of Engineering and Natural Sciences, Tampere University, Korkeakoulunkatu 8, FI-33720 Tampere, Finland

[4]Research Organization of Science and Technology, Ritsumeikan University, Kusatsu, Shiga 525-8577, Japan

[5]Display Research Center, Samsung Display, 1 Samsung-ro, Giheung-gu, Yongin-si, Gyeonggi-do, 17113 Korea

[6]SANKEN (The Institute of Scientific and Industrial Research), Osaka University, 8-1 Mihogaoka, Ibaraki, Osaka 567-0047, Japan

E-mail: sakai@chem.keio.ac.jp, hyeondeuk.kim@samsung.com, sakamoto@sanken.osaka-u.ac.jp

Abstract

Singlet exciton fission (SF) is one of the limited options for exceeding the theoretical limit of solar energy utilisation, the so-called Shockley–Queisser limit. Thus, improving endothermic SF efficiency will significantly contribute to the efficient utilisation of solar energy beyond the existing technology. In this regard, combining SF molecules with quantum dots (QDs) has achieved excellent results. However, the factors underlying the enhanced SF efficiency remain poorly understood. Herein, we discovered that inter-material orbital hybridisation between SF molecules and QDs harnesses endothermic SF. Theoretical calculations and transient absorption measurements of tetracene (Tc)–CdX (X = Te, Se, S) QD composites showed that multiple orbital hybrid levels formed by orbital hybridisation act as intermediate levels to facilitate SF. This result sheds light on alternative factors affecting SF efficiency beyond the molecular packing of SF molecules on the QD surface. The synergy effect on the zero-dimensional molecular assembly on QDs will provide guidance for the development of organic-inorganic hybrid solar cells, which overcome the Shockley–Queisser limit.

Singlet exciton fission (SF), a physical phenomenon that produces two excitons from one photon, is one of the limited options for exceeding the theoretical limit of solar energy

utilisation, the so-called Shockley–Queisser limit[1-6]. An endothermic SF process, in which one singlet exciton (S_1) generates two triplet excitons (T_1) with a total energy greater than that of S_1, is difficult from an energetic point of view, and its reverse reaction cannot be avoided. However, most of the SF molecules that can generate T_1 energy applicable to Si solar cells fall into this category. Overcoming this endothermic process has been a major challenge in SF research[3, 7-12]. Developing a versatile strategy for improving endothermic SF efficiency will significantly contribute to the application of SF and pave the way for efficient utilisation of solar energy beyond the existing technology.

In this regard, combining SF molecules with quantum dots (QDs) has achieved excellent results[13, 14]. QDs are an important class of materials with tuneable optical properties[15]. Their large specific surface area allows the integration of numerous molecules on the surface[16, 17]. Efficiencies close to 200% of the theoretical limit have been realised using molecule-QD composites[14]. Endothermic SF on a QD is expected to be highly efficient without exception. In their pioneering work in 2018, Rao et al. indirectly proposed the progression of efficient endothermic SF from the increase in emission intensity of PbS in a PbS–tetracene (Tc) complex[18]. Furthermore, they speculated that the Tc configuration on the PbS surface plays a key role in SF. However, elucidating the SF process on the PbS surface is quite difficult because the selective excitation of molecules on a QD with a narrow band gap is impossible, and triplet excitons generated via SF move to the QD owing to energy transfer.

Herein, we investigated the endothermic SF of Tc on the surfaces of CdS, CdSe, and CdTe QDs via the selective excitation of Tc by transient absorption (TA) spectroscopies at different time scales. Furthermore, the factors underlying SF efficiency were determined by theoretical calculations. Although the mechanism of endothermic SF has been an area of active debate, the involvement of a multi-excitonic (ME) state is considered an influential mechanism. In the ME mechanism, the endothermic process is overcome by the formation of spurious bands by SF molecules in the single crystal. The results indicated that hybridisation of the orbitals of SF molecules and QDs forms an alternative state harnessing this endothermic SF process with high efficiency. This finding sheds light on an alternative mechanism of SF beyond the classical one based on molecular packing.

Results

Materials design

QDs (CdS, CdSe, and CdTe) were selected as a scaffold for Tc integration for efficient SF (See also the sample preparation and characterization section in the Supplementary Information (SI)). The computationally optimised structures of Tc on CdTe and CdSe and schematic illustration of the relevant photophysical processes of SF on QD–Tc is displayed in Fig. 1a and b, respectively [see also the Computational method in the SI]. The selective photoexcitation of Tc on a QD generates a singlet excited state [Tc(S_1)], which then undergoes endothermic SF with a neighbouring Tc molecule to produce an ME state, as described in detail in the Discussion section (See also the Transient absorption measurement section in the SI). The ME state, also referred to as a correlated triplet pair, separates into two triplet excitons (Tc(T_1)). In the case of CdTe–Tc, orbital hybridisation between CdTe and Tc produces an intermediate hybridised state (HS) that improves SF efficiency.

Sample preparation and characterisation

The QDs were synthesised using a hot injection method and dissolved in hexane[14, 16, 17]. The transmission electron microscopy images indicated that the sizes of the CdS, CdSe, and CdTe QDs are 2.7, 2.8, 2.8 nm, respectively (Supplementary Fig. 7). The X-ray diffraction patterns indicated that the CdS, CdSe, and CdTe QDs have a zinc blende crystal structure (JCPDS Nos. 06-3897, 19-0191, and 15-0770, respectively) (Supplementary Fig. 8).

The QDs exhibited exciton peaks depending on their composition and size because of the shift in the band gap of QDs reflect the quantum size effect and composition (Fig. 1c). Tc showed characteristic absorption and fluorescence peaks at 540 and 545 nm, respectively (Fig. 1c,d and Supplementary Fig. 9). The absorption of QD–Tc reflected those of both Tc and QD, indicating that Tc is attached to the QD surface. This attachment through a carboxylic acid group occurs via a ligand exchange reaction. Tc, which is not coordinated to the QD surface, was then completely removed via gel permeation chromatography before the

experiment[16, 17]. The average number of Tc molecules on a single QD (*n*) was quantitatively controlled by changing the Tc concentration during the ligand exchange reaction. We synthesised QDs attached to a similar number of Tc molecules with a similar molecular orientation (see Characterization section in the SI for details).

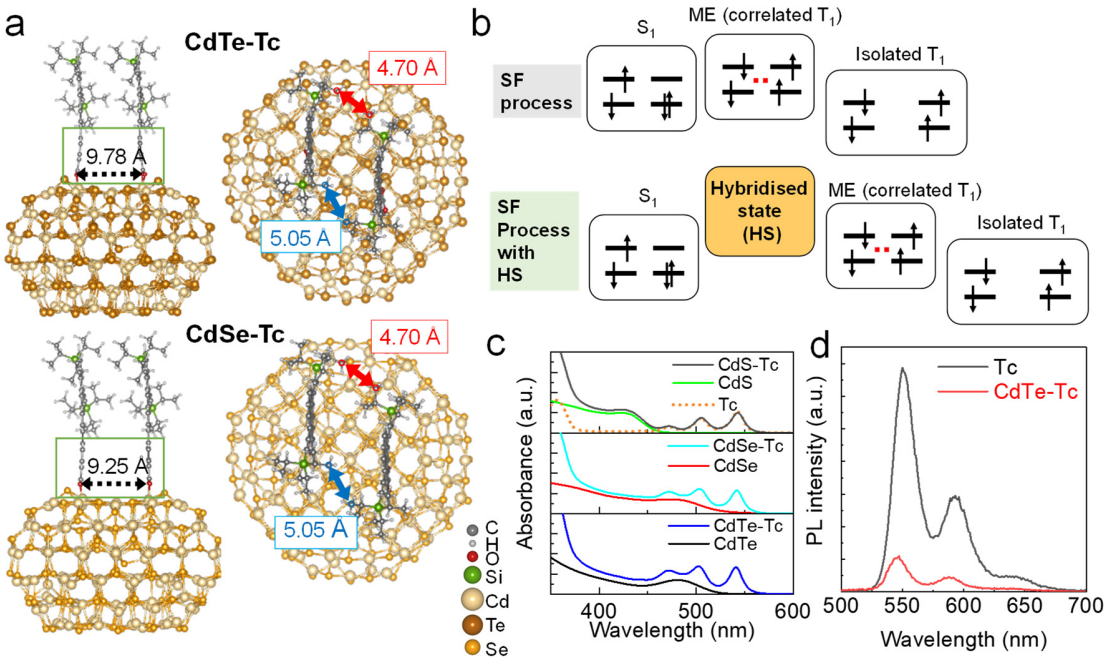

Fig. 1 | Singlet exciton fission (SF) mechanism of tetracene (Tc) on quantum dots (QDs). **a**, Optimised structures of Tc on CdTe [$Cd_{163}Te_{163}$] and CdSe [$Cd_{163}Se_{163}$] in the ground state calculated by density functional theory (Supplementary Fig. 15 for details). **b**, Schematic illustration of SF at the QD–Tc heterointerface. The selective excitation of Tc forms a molecular singlet exciton (S_1), which then undergoes SF to produce two triplet excitons (T_1) via both a hybridised state (HS) and multi-excitonic (ME) state in the case of CdTe–Tc and only an ME state in the case of CdSe–Tc. **c**, UV–visible absorption spectra of CdTe–Tc, CdSe–Tc, CdS–Tc, and Tc in toluene. **d**, PL spectra of Tc and CdTe–Tc under 400 nm excitation.

The photoluminescence (PL) spectra of Tc and CdTe–Tc are shown in Fig. 1d. The photoluminescence quantum yield (PLQY) of Tc was dramatically damped (0.29% and 0.012% for free Tc and CdTe–Tc, respectively, see also Supplementary Table 1 and Supplementary Fig. 10) by dense packing on the QD surface, indicating that most Tc(S_1) was consumed by SF. No bleaching of QD absorption, indicating energy or carrier transfer to QD, was observed in the TA measurements (vide infra).

Femtosecond transient absorption (fs-TA) measurements

To investigate the QD dependence of SF efficiency, we conducted fs-TA measurements of the QD–Tc systems. The two-dimensional (2D) fs-TA maps of the Tc-coordinated QDs are displayed in Fig. 2a,d,g. Tc on the QDs was selectively excited by a laser pulse with a wavelength of 540 nm, where the QDs do not show absorption. Upon the excitation of Tc on CdTe, excited-state absorption, which is characteristic of the singlet excited state (Tc(S_1)) in Tc, was observed at approximately 450 nm. Following the decay of Tc(S_1), the TA signal assigned to the ME state (i.e., correlated triplet pair state) emerged, indicating that SF occurred on CdTe–Tc. The assignment of the TA of the ME state was also supported by the fs-TA spectra of CdTe–Tc with different numbers of Tc molecules (Supplementary Fig. 12). An ME state was observed for the CdTe–Tc with a larger number of Tc molecules (i.e., densely packed Tc). In contrast, the yield of the ME state in CdTe-Tc decreased together with a decrease in the number of Tc molecules (i.e. sparsely packed Tc) (Supplementary Table 2). The typical TA spectrum of individual triplet state T_1 was observed in the case of CdTe–Tc with a smaller number of Tc molecules (i.e., sparsely packed Tc).

The difference in QDs resulted in a dramatic shift in the SF process. For CdSe–Tc and CdS–Tc, a similar ME generation was observed after the excitation of Tc by the 540 nm laser. However, the yield of the generated ME state was small (Table 1). These results indicate that the mechanism of SF on the QD–Tc significantly depends on the scaffold. The kinetics of SF processes were further analysed using global fitting analysis.[19]

Table 1 | Photoluminescence quantum yield (PLQY) and multi-excitonic (ME) and triplet yields of quantum dot–tetracene (Tc) systems

Sample	PLQY (%)	Φ_{ME} (%)	Φ_T (%)
CdTe–Tc	0.012	196	95
CdSe–Tc	0.016	156	66
CdS–Tc	0.021	141	53

Global fitting analysis

In the global fitting analysis shown in Fig. 2b, the three evolution-associated spectra suggest the occurrence of SF on CdTe–Tc. The component with a lifetime of 11 ps represents Tc(S_1) with a unique peak at 440 nm (Fig. 2c). A component spectrum (119 ps) corresponding to the HS state was observed, which is a TA spectrum similar in shape to the spectrum corresponding to S_1 but with a different lifetime.[20] The final component with a lifetime of >5000 ps corresponds to the ME state.

Generally, an intermediate species of Tc in the SF process, such as a charge transfer (CT) state, shows a similar spectrum to that of S_1[19]. Therefore, separating S_1 and this intermediate species is very difficult. However, kinetic analysis revealed a specific intermediate species on CdTe–Tc. The relation between the unity SF yield and existence of this intermediate state indicates that the unique intermediate plays a key role in the SF process on CdTe–Tc. We call this intermediate state HS for clarity. It should be noted that the HS was only observed for CdTe–Tc. No such intermediate was observed for either CdSe–Tc or CdS–Tc.

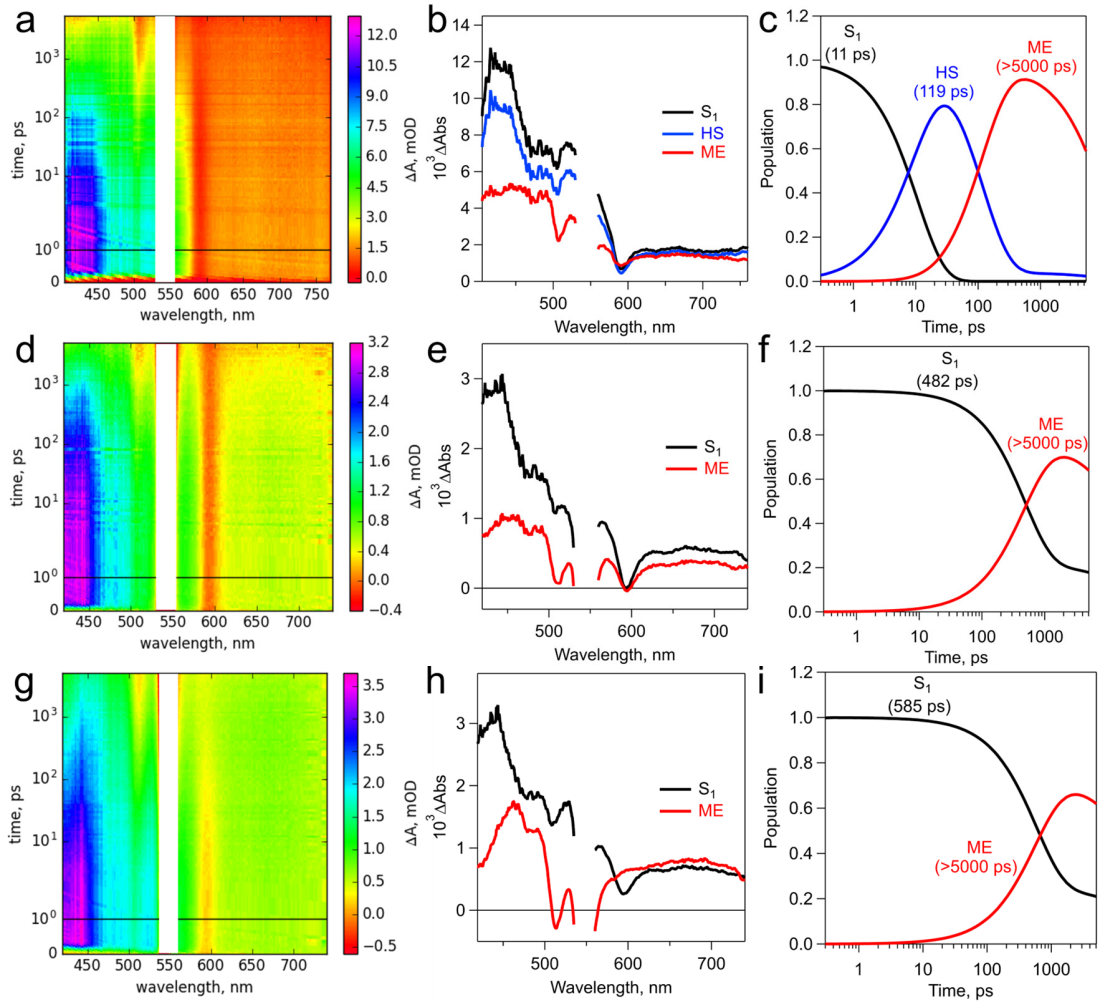

Fig. 2 | Femtosecond transient absorption (fs-TA) measurements of quantum dot (QD) –tetracene (Tc) systems pumped at 540 nm. a, **d**, **g**, Two-dimensional fs-TA maps of CdTe–Tc (**a**), CdSe–Tc (**d**), and CdS–Tc (**g**). **b**, **e**, **h**, Global fitting analysis of the TA spectra of CdTe–Tc (**b**), CdSe–Tc (**e**), and CdS–Tc (**h**). **c**, **f**, **i**, Population dynamics of CdTe–Tc (**c**), CdSe–Tc (**f**), and CdS–Tc (**i**). Singlet (S_1) Tc is quenched by singlet exciton fission (SF), generating a multi-excitonic (ME) state (i.e., correlated triplet pair).

Picosecond transient absorption (ps-TA) measurements

The fate of the ME state on the QD–Tc surface was investigated by performing ps-TA measurements (Fig. 3). For all QD–Tc systems, the absorption of the ME peak at approximately 450 nm was observed upon 540 nm laser excitation. The absorption spectrum gradually shifted to that of the typical triplet state (Tc(T_1)). This result clearly indicates that the SF of Tc on the QDs generate the ME state in the nanosecond region, which can finally be separated as an individual T_1 state. Global fitting analysis of the ps-TA spectra of the QD–Tc systems is shown in Fig. 3b,e,h. The decay of the ME states of CdTe–Tc and CdSe–Tc at 440 nm coincided with the rise of individual Tc(T_1), indicating that the ME state separates to form Tc(T_1) with an efficiency of almost unity in the picosecond region. CdTe–Tc and CdSe–Tc showed negligible PL in this time region (Supplementary Fig. 13). This result strongly supports that recombination from ME or T_1 is a minor process.

The femtosecond-to-picosecond time-resolved shift of the TA signals verified the occurrence of SF between Tc molecules on the QD surface. The proposed SF mechanism is illustrated in Fig. 1b. The ME and triplet yields of SF on CdTe–Tc were 196% and 95%, respectively. Tc coordinated to CdTe showed an almost unity SF. On the other hand, the ME and triplet yields of SF on CdSe–Tc were 156% and 66%, respectively. Thus, SF efficiency was dramatically reduced on the CdSe surface. Furthermore, the ME and triplet yields of SF on CdS–Tc were 141% and 53%, respectively. Evidently, the interposition of the HS as an intermediate state increases the ME yield while suppressing the reverse reaction from the ME. Thus, the existence of the HS in CdTe–Tc significantly improves SF efficiency.

The nanosecond transient absorption (ns-TA) spectra showed that Tc(T_1) generated on the CdTe QD surface had a lifetime of 66 μs (Supplementary Fig. S14), which is much longer than the previously reported values for crystalline solids and covalent dimers of Tc.[21] Kinetic analysis of the decay profile of Tc(T_1) showed that the decay corresponding to the back reaction (i.e., triplet–triplet annihilation) was negligible. The estimated triplet yield of SF from the long-lived component of the ns-TA spectrum was 95%, indicating that almost no back reaction occurred even in the millisecond region. Prevention of the back reaction was similarly observed for pentacene derivatives coordinated to CdTe QDs[14]. A non-conjugated

arrangement of Tc on the CdTe surface provides a through-space interaction for SF, which would prevent undesired deactivation processes.

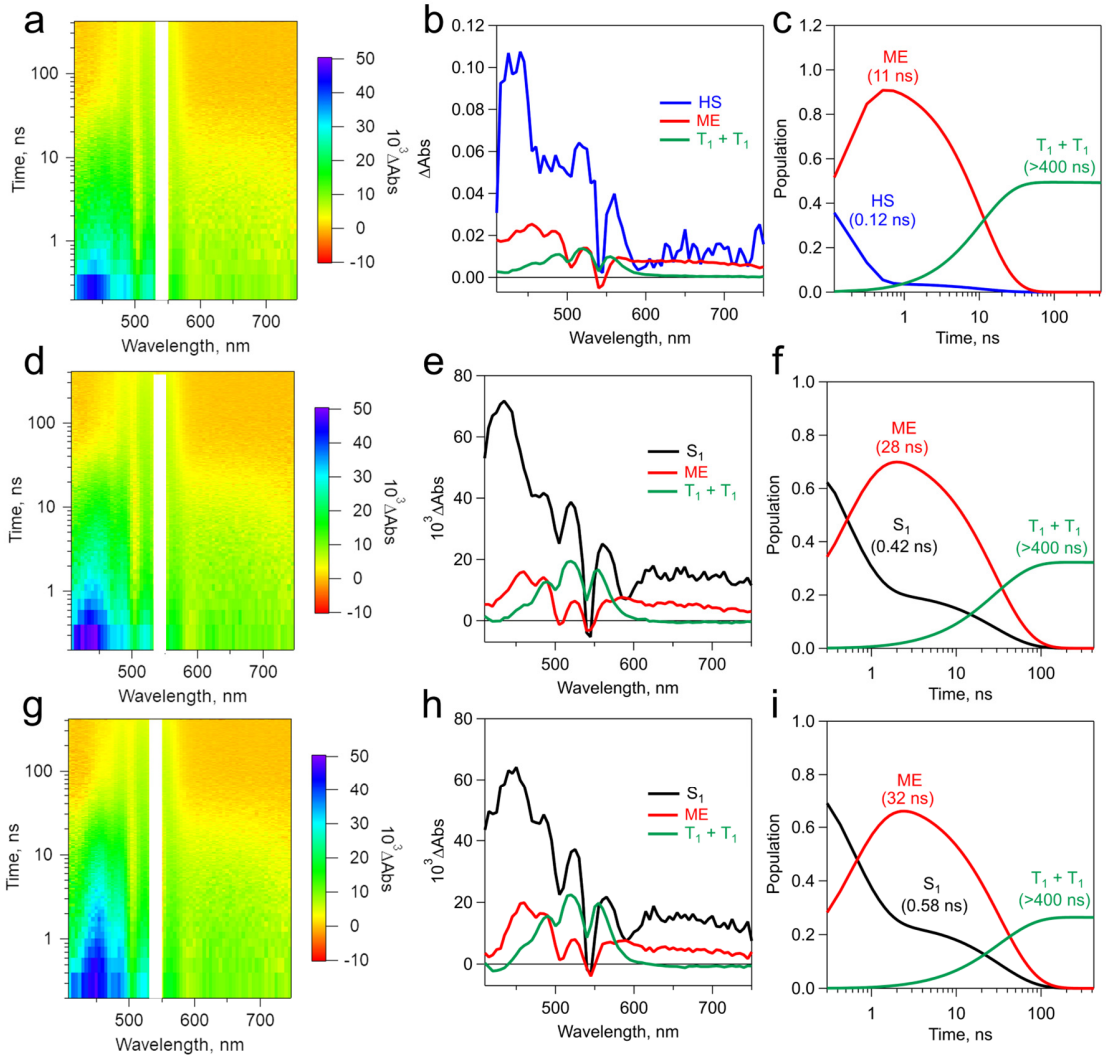

Fig. 3 | Picosecond transient absorption (ps-TA) measurements of quantum dot (QD)–tetracene (Tc) systems pumped at 540 nm. a, **d**, **g**, Two-dimensional ps-TA maps of CdTe–Tc (**a**), CdSe–Tc (**d**), and CdS–Tc (**g**). **b**, **e**, **h**, Global fitting analysis of the TA spectra of CdTe–Tc (**b**), CdSe–Tc (**e**), and CdS–Tc (**h**). **c**, **f**, **i**, Population dynamics of CdTe–Tc (**c**), CdSe–Tc (**f**), and CdS–Tc (**i**).

Computational geometry optimisation of Tc molecules on a QD

Among the factors influencing the mechanism and efficiency of SF, molecular orientation is believed to have the most impact. We evaluated the change in molecular orientation in the excited state caused by QDs using computer simulations.

Ab initio calculations of $[Cd_{163}Te_{163}+2\ Tc]^{2-}$ and $[Cd_{163}Se_{163}+2\ Tc]^{2-}$ demonstrated the structural rearrangement of a Tc pair on the QD surface, especially at the ligating benzoate groups. We conducted the structural optimisation of the Tc pair on a pre-optimised $Cd_{163}X_{163}$ (X = Te or Se) surface (Fig. 1a, Supplementary Fig. 15a,c, and section 4 in the SI). After geometry optimisation, the two Tc molecules were parallel to each other and attached to the $Cd_{163}X_{163}$ (X = Te or Se) surface through their carboxylate ligands. Considering that the Cd–Te bond (3.24 Å) is longer than the Cd–Se bond (3.04 Å), the C–C distance between the bottom carboxylate ligands of the two Tc molecules was larger in CdTe–Tc (9.78 Å) than in CdSe–Tc (9.25 Å) (Fig. 1a and Supplementary Fig. 15). Notably, the structures of the top parts of the right and left Tc molecules were almost identical, as well as the intermolecular distances in $[Cd_{163}Te_{163}+2\ Tc]^{2-}$ and $[Cd_{163}Se_{163}+2\ Tc]^{2-}$. The strong π–π interaction between the Tc pair resulted in convergence to a similar configuration in both cases despite the different geometrical configurations of the bottom benzoate groups.

The main difference between the Tc pairs in $[Cd_{163}Te_{163}+2\ Tc]^{2-}$ and $[Cd_{163}Se_{163}+2\ Tc]^{2-}$ was the bending angle of the bottom benzoate groups (Supplementary Fig. S15b,d). The root-mean-square displacements (RMSDs) of the bottom benzoate groups of the right and left Tc molecules (indicated by the pink dotted square in Supplementary Fig. 15a,c) were 0.152 and 0.109 Å for $[Cd_{163}Te_{163}+2\ Tc]^{2-}$ and $[Cd_{163}Se_{163}+2\ Tc]^{2-}$, respectively. The RMSD is larger for $[Cd_{163}Te_{163}+2\ Tc]^{2-}$ than for $[Cd_{163}Se_{163}+2\ Tc]^{2-}$ because the mismatch of the distance between the carboxylate ligands of the Tc pair and that between the binding sites on the QD surface, which is related to the Cd–X (X = Te or Se) bond length, is greater in the former than in the latter.

In general, SF is enhanced when there is appropriate structural deviation between molecules. The greater bending of the bottom benzoate groups in $[Cd_{163}Te_{163}+2\ Tc]^{2-}$, which causes structural deviation between the right and left Tc molecules, can accelerate SF. In contrast, the bending is less significant in $[Cd_{163}Se_{163}+2\ Tc]^{2-}$ and the right and left Tc molecules are closer, leading to suppressed SF. The structural deviation between the right and left Tc molecules was maintained in the excited states of both $[Cd_{163}Te_{163}+2\ Tc]^{2-}$ and $[Cd_{163}Se_{163}+2\ Tc]^{2-}$ (Supplementary Figs. 21–23). However, the difference between the RMSDs of the right and left Tc molecules in $[Cd_{163}Te_{163}+2\ Tc]^{2-}$ and $[Cd_{163}Se_{163}+2\ Tc]^{2-}$ was only 0.043 Å, which cannot fully rationalise the difference between the SF efficiencies of CdTe–Tc and CdSe–Tc. The nuclear magnetic resonance (NMR) results indicate that the ligand number ratio of Tc is similar regardless of the QDs (See SI for characterization section 2-3), which support the computational simulations.

Orbital analysis

We performed ab initio orbital calculations of excited-state $[Cd_{163}Te_{163}+2\ Tc]^{2-}$ and $[Cd_{163}Se_{163}+2\ Tc]^{2-}$ to investigate the perturbation between the QDs and Tc (see section 4 in the SI). To facilitate discussion of the interaction between the molecular and QD orbitals, the orbitals are numbered in Fig. 4 and Supplementary Figs. 16–19.

The lowest-energy state of $[Cd_{163}Te_{163}+2\ Tc]^{2-}$ is the Tc excited state [Tc(S_1)], where both the excited electron and excited hole are located around the right Tc, as the orbital shapes of #1733α and #1717α show, respectively. Orbital #1733α is a QD–Tc hybrid orbital where the excited electron is delocalised over the right Tc and QD (i.e., HS). Remarkably, the energy difference between #1733α–#1736α related to the excited electron is only approximately 0.028 eV and, considering the orbital energy fluctuation and thermal energy at ambient temperature, the excited electron should be able to hop among these orbitals. This implies that the excited electron can appear effectively in both the right and left Tc molecules by utilising the QD–Tc hybrid orbitals at ambient temperature. Orbital #1717α is also a QD–Tc hybrid orbital where the excited hole is delocalised over the right Tc and QD. The energy difference between #1714α, #1715α, #1717α, and #1718α related to the excited hole is only

approximately 0.014 eV. Considering the orbital energy fluctuation and thermal energy at finite temperature, the excited hole should also be able to hop among these orbitals. Thus, the QD–Tc hybrid orbitals allow the excited hole to effectively exist both in the right and left Tc molecules.

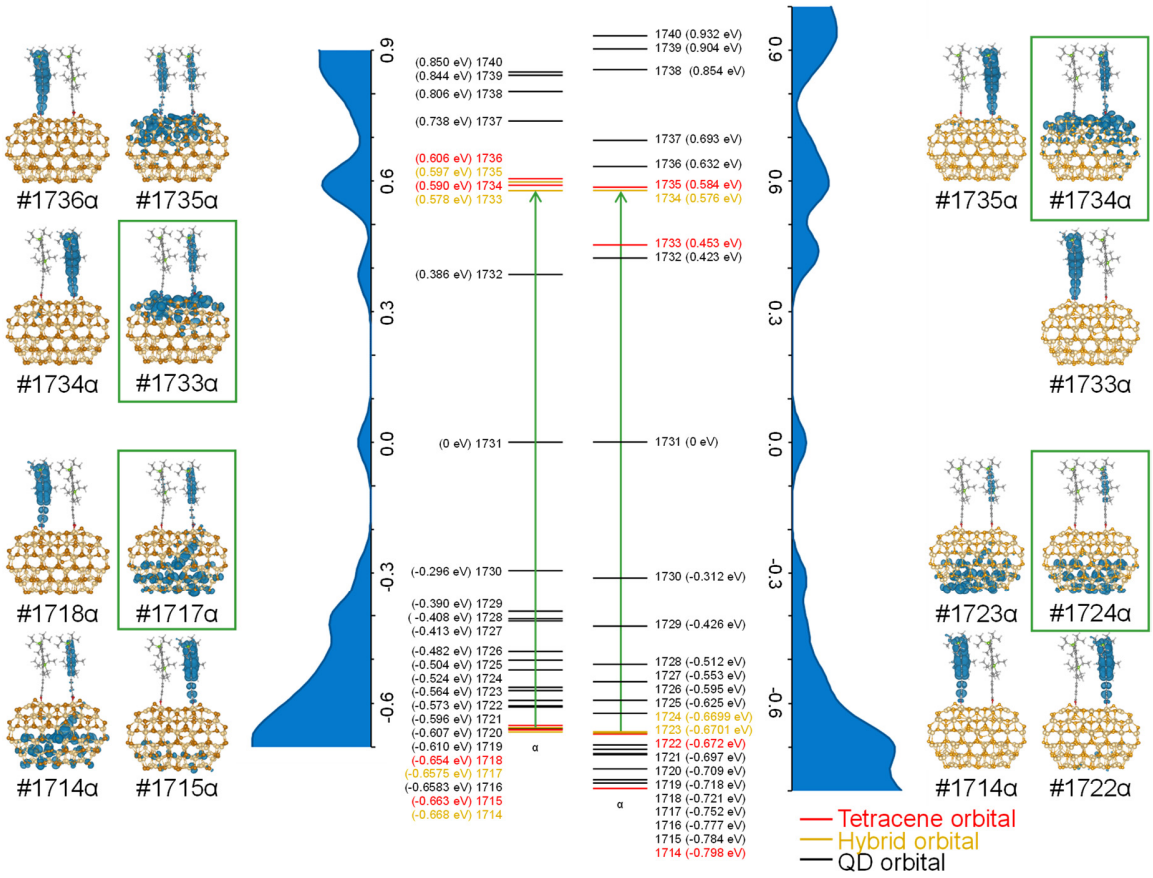

Fig. 4 | Orbital energy diagrams of $[Cd_{163}Te_{163}+2Tc]^{2-}$ and $[Cd_{163}Se_{163}+2Tc]^{2-}$ in the excited state. The energy levels of tetracene (Tc), the quantum dots (QDs), and their hybrid α-orbitals are shown as red, black, and yellow lines, while the smoothened density of state curves are shown in blue. Tc-related orbitals are graphically shown on both sides with those containing an excited electron or excited hole surrounded by a green frame. There is no electronic excitation in the β-orbitals.

The effective hopping between the right and left Tc molecules induces CT states, where the excited electron and excited hole are located not in the same Tc molecule but in different Tc molecules: When the initially excited electron hops to #1735α or #1736α while the initially excited hole stays at #1717α, such excited state corresponds to a CT state. It should be emphasised that the energetically close QD–Tc hybrid orbitals provide more CT states by facilitating hopping to the CT states, which increases the probability of transition to the CT states and should enhance SF. We note that, if the QD–Tc hybrid orbitals are not energetically close and impossible to utilise, there would only be one available CT state where the excited electron and excited hole are completely localised on only one of the Tc molecules.

The lowest-energy state of $[Cd_{163}Se_{163}+2\ Tc]^{2-}$ is also the Tc excited state [Tc(S_1)], where both the excited electron and excited hole are located around the right Tc, as the orbital shapes of #1734α and #1724α show, respectively. Orbital #1734α is a QD–Tc hybrid orbital where the excited electron is delocalised over the right Tc and QD. However, the number of Tc-related orbitals is 3, which is smaller than that in $[Cd_{163}Te_{163}+2\ Tc]^{2-}$, and the energy difference between #1733α–#1735α (~0.123 K) is too large to hop. Therefore, $[Cd_{163}Se_{163}+2\ Tc]^{2-}$ cannot effectively utilise the QD–Tc hybrid orbital even at ambient temperature, causing the excited electron to be localised on only one side of the Tc pair at all times. Orbital #1724α, where the excited hole is located, is also a QD–Tc hybrid orbital. However, the electronic density of the excited hole is smaller than that in $[Cd_{163}Te_{163}+2Tc]^{2-}$. In addition, the large energy difference (~0.126 K) between #1714α and #1722α–#1724α makes it difficult for the excited hole to hop from the initially excited right Tc to the left Tc.

Discussion

The fs-TA spectra revealed a pronounced QD dependence of endothermic SF efficiency. Because SF efficiency is generally affected by molecular configuration, we initially believed that the difference in molecular configuration causes QD dependence. However, the NMR and computational simulation results showed no significant difference in the number and molecular configuration of Tc on CdTe and CdSe. Therefore, the QD dependence of SF efficiency is due to factors other than molecular packing on the QD surface.

Density functional theory calculations indicated that the intermediate CT state is an excited state formed by the excited electron on one Tc and the excited hole on the other Tc. Such a CT state can be induced by hybridising the Tc and QD orbitals (i.e., HS). In the fs-TA spectrum, HS was observed independently of the number of Tc molecules on CdTe (Supplementary Fig. 12), indicating that HS is not due to an intermolecular interaction but a perturbation between the QD and molecule.

In a single crystal, the increase in the density of state (DOS) due to orbital overlap between Tc molecules in the ME state is the key to promoting SF in Tc[22]. By exploiting the QD–Tc hybrid orbitals, the Tc-related DOS effectively increases and becomes denser, which leads to an overwhelming improvement in SF efficiency, especially in CdTe.

The SF processes in QD–Tc is summarised in Fig. 1b and Supplementary Scheme 1. (1) When Tc is photoexcited, S_1 is formed. (2) In the case of CdTe, S_1 forms the ME state through the HS. (3) The formed ME state generates an isolated T_1 with almost 100% efficiency. In contrast, for CdSe and CdS, the ME state is formed directly from S_1. This process is rather slower than the formation of the QD–Tc hybrid orbital state; thus, competition with radiative and non-radiative transitions from S_1 leads to a loss in SF efficiency. The difference between CdTe–Tc, CdSe–Tc, and CdS–Tc is due to the difference in the DOS of the QDs. CdTe–Tc, with a large lowest unoccupied molecular orbital of Tc and large orbital overlap, is the most likely to create a hybrid orbital state. Based on the PL results, the reverse reaction from the ME state or individual T_1 is very minor process. The key to high efficiency is the dominance of the event that progresses at the earliest stage, which can be interrupted by the presence of an intermediate level. It is expected that a similar phenomenon will occur in other suitable molecules and QDs combination. The discovered synergy effect will provide important guidance for the development of organic-inorganic hybrid energy conversion systems, which overcome the Shockley–Queisser limit.

Data Availability

The data sets within the article and Supplementary Information are available from the authors upon reasonable request.

Acknowledgements

This work was supported by the Japan Society for the Promotion of Science Grants-in-Aid for Scientific Research (A) (KAKENHI) (grant no. JP21H04638) (M.S.) and Japan Science and Technology Agency Fusion Oriented Research for disruptive Science and Technology (FOREST) program (grant no. PMJFR201M) (M.S.) and the Japan Society for the Promotion of Science Grants-in-Aid for Scientific Research (C) (KAKENHI) (grant no. JP23K04708 and grant no. JP20K05652) (H.S.), JSPS KAKENHI Grant-in-Aid for Transformative Research Areas, "Dynamic Exciton", grant no. JP20H05840 (H.K.), and JSPS Core-to-Core Program, grant no. JPJSCCA20220004 (H.K.). The authors deeply appreciate Prof. Nikolai V. Tkachenko for his advice on the SF mechanism, kinetic analysis, and TA measurements.

Author contributions

M.S. conceived the concept of this work. M.S. and conceived and designed experiments related to material fabrication. H.S. and M.S. conceived and designed the experiments related to spectroscopic measurements and analysis. J.Z. performed the syntheses of QDs and QD–Tc systems. H.S., T.H., and R.K. performed the TA experiments. K.S. and H.K. performed the NMR experiments. K.H.D. and I.-Y.C. carried out the theoretical calculation. M.S., H.S. and K.H.D. wrote the paper. All authors participated in the discussion of the research.

Competing interests

The authors declare no competing interests.

Additional information

Supplementary information The online version contains supplementary material available at https://XXXX.

REFERENCES

1. Daiber, B., Maiti, S., Ferro, S. M., Bodin, J., van den Boom, A. F. J., Luxembourg, S. L., Kinge, S., Pujari, S. P., Zuilhof, H., Siebbeles, L. D. A. & Ehrler, B. Change in tetracene polymorphism facilitates triplet transfer in singlet fission-sensitized silicon solar cells. *J. Phys. Chem. Lett*. **11**, 8703–8709 (2020).
2. Smith, M. B. & Michl, J. Singlet fission. *Chem. Rev.* **110**, 6891–6936 (2010).
3. Wang, Z., Liu, H., Xie, X., Zhang, C., Wang, R., Chen, L., Xu, Y., Ma, H., Fang, W., Yao, Y., Sang, H., Wang, X., Li, X. & Xiao, M. Free-triplet generation with improved efficiency in tetracene oligomers through spatially separated triplet pair states. *Nat. Chem.* **13**, 559–567 (2021).
4. Jones, A. C., Kearns, N. M., Ho, J.-J., Flach, J. T. & Zanni, M. T. Impact of non-equilibrium molecular packings on singlet fission in microcrystals observed using 2D white-light microscopy. *Nat. Chem.* **12**, 40–47 (2020).
5. Pun, A. B., Asadpoordarvish, A., Kumarasamy, E., Tayebjee, M. J. Y., Niesner, D., McCamey, D. R., Sanders, S. N., Campos L. M. & Sfeir, M. Y. Ultra-fast intramolecular singlet fission to persistent multiexcitons by molecular design. *Nat. Chem.* **11**, 821–828 (2019).
6. Einzinger, M., Wu, T., Kompalla, J. F., Smith, H. L., Perkinson, C. F., Nienhaus, L., Wieghold, S., Congreve, D. N., Kahn, A., Bawendi, M. G. & Baldo, M. A. Sensitization of silicon by singlet exciton fission in tetracene. *Nature* **571**, 90–94 (2019).
7. Stern, H. L., Cheminal, A., Yost, S. R., Broch, K., Bayliss, S. L., Chen, K., Tabachnyk, M., Thorley, K., Greenham, N., Hodgkiss, J. M., Anthony, J., Head-Gordon, M., Musser, A. J., Rao, A. & Friend, R. H. Vibronically coherent ultrafast triplet-pair formation and subsequent thermally activated dissociation control efficient endothermic singlet fission. *Nat. Chem.* **9**, 1205–1212 (2017).
8. Sanders, S. N. & Campos, L. M. A birds-eye view of the uphill landscape in endothermic singlet fission. *Chem* **3**, 536–538 (2017).
9. Rao, A. & Friend, R. H. Harnessing singlet exciton fission to break the Shockley–Queisser limit. *Nat. Rev. Mat.* **2**, 17063 (2017).
10. Burdett, J. J. & Bardeen, C. J. The dynamics of singlet fission in crystalline tetracene and covalent analogs. *Acc. Chem. Res.* **46**, 1312–1320 (2013).
11. Chan, W.-L., Ligges, M. & Zhu, X.-Y. The energy barrier in singlet fission can be overcome through coherent coupling and entropic gain. *Nat. Chem.* **4**, 840–845 (2012).
12. Burdett, J. J., Müller, A. M., Gosztola, D. & Bardeen, C. J. Excited state dynamics in solid and monomeric tetracene: the roles of superradiance and exciton fission. *J. Chem. Phys.* **133**, 144506 (2010).
13. Lu, H., Chen, X., Anthony, J. E., Johnson, J. C. & Beard, M. C. Sensitizing singlet fission with perovskite nanocrystals. *J. Am. Chem. Soc.* **141**, 4919–4927 (2019).
14. Zhang, J., Sakai, H., Suzuki, K., Hasobe, T., Tkachenko, N. V., Chang, I.-Y., Hyeon-Deuk, K., Kaji, H., Teranishi, T. & Sakamoto, M. Near-unity singlet fission on a

quantum dot initiated by resonant energy transfer. *J. Am. Chem. Soc.* **143**, 17388–17394 (2021).
15. Lian, Z., Kobayashi, Y., Vequizo, J. J. M., Ranasinghe, C. S. K., Yamakata, A., Nagai, T., Kimoto, K., Kobayashi, K., Tanaka, K., Teranishi, T. & Sakamoto, M. Harnessing infrared solar energy with plasmonic energy upconversion. *Nat. Sustainability* **5**, 1092–1099 (2022).
16. Zhang, J., Kouno, H., Yanai, N., Eguchi, D., Nakagawa, T., Kimizuka, N., Teranishi, T. & Sakamoto, M. Number of surface-attached acceptors on a quantum dot impacts energy transfer and photon upconversion efficiencies. *ACS Photonics* **7**, 1876–1884 (2020).
17. Zhang, J., Chiga, Y., Kouno, H., Yanai, N., Kimizuka, N., Teranishi, T. & Sakamoto, M. Exciton recycling in triplet energy transfer from a defect-rich quantum dot to an organic molecule. *J. Phys. Chem. C* **126**, 11674–11679 (2022).
18. Davis, N. J. L. K., Allardice, J. R., Xiao, J., Petty II, A. J., Greenham, N. C., Anthony, J. E. & Rao, A. Singlet fission and triplet transfer to PbS quantum dots in TIPS-tetracene carboxylic acid ligands. *J. Phys. Chem. Lett.* **9**, 1454–1460 (2018).
19. Snellenburg, J. J., Laptenok, S., Seger, R., Mullen, K. M., & van Stokkum, I. H. M. Glotaran: A Java-Based Graphical User Interface for the R Package TIMP. *J. Stat. Softw.*, **49**(3), 1–22 (2012).
20. Tang, Z., Zhou, S., Liu, H., Wang, X., Liu, S., Shen, L., Lu, X. & Li, X. Tuning singlet fission in amphipathic tetracene nanoparticles by controlling the molecular packing with side-group engineering. *Mater. Chem. Front.* **4**, 2113–2125 (2020).
21. Burdett, J. J. & Bardeen, C. J. Quantum beats in crystalline tetracene delayed fluorescence due to triplet pair coherences produced by direct singlet fission. *J. Am. Chem. Soc.* **134**, 8597–8607 (2012).
22. Sanders, S. N., Pun, A. B., Parenti, K. R., Kumarasamy, E., Yablon, L. M., Sfeir, M. Y. & Campos, L. M. Understanding the bound triplet-pair state in singlet fission. *Chem* **5**, 1988–2005 (2019).